Seismic Hazard Evaluation of RC Buildings in İzmir after The Aegean Sea Earthquake on October 30, 2020

Halit Cenan Mertol[1], Gokhan Tunc[1] & Tolga Akis[1]

[1]Civil Engineering Department, Atilim University, Ankara, Turkey

***Corresponding author**: Halit Cenan Mertol, cenan.mertol@atilim.edu.tr*

SEISMIC HAZARD EVALUATION OF RC BUILDINGS IN IZMIR AFTER THE AEGEAN SEA EARTHQUAKE ON OCTOBER 30, 2020

Abstract

An earthquake with a magnitude of M_w = 6.6 and a depth of approximately 16.5 kilometers occurred on October 30, 2020, off the cost of Samos, a Greek island 35 kilometers southwest of Seferihisar, a town in İzmir, located in the western part of Turkey. The earthquake caused several collapses and severe structural damage in close to 6,000 buildings, specifically in the Bayraklı District in İzmir Bay. This study presents the observations and findings of a technical team that visited the earthquake-affected areas right after the earthquake. According to site observations, it was found out that almost all of the collapsed or severely damaged reinforced concrete buildings in the region were built between 1975 and 2000. The site observations also confirmed that the construction of these collapsed or damaged buildings did not conform with the requirements outlined in the Turkish Earthquake Codes used at the time. The failures and severe damage of the buildings in the earthquake-affected area are mainly related to inadequate reinforcement configuration, poor material quality, the absence of geotechnical studies, and framing problems related to their lateral load carrying systems. It is, therefore, recommended that all the buildings located in and around İzmir Bay, especially those built between 1975 and 2000, be structurally evaluated to prevent any further loss of life and property during future earthquakes.

Key words: structural failure, reinforced concrete buildings, 2020 Aegean Sea earthquake, İzmir.

1 Introduction

Turkey lies in one of the most active earthquake zones. Based on statistical studies, in Turkey, a strong earthquake with a magnitude of M_w between 6.0 and 6.9 occurs every two years, and a major one with a magnitude M_w of above 6.9 occurs every three years. Approximately 98% of the Turkish population lives in earthquake-risk designated areas. Since the establishment of the Turkish Republic in 1923, approximately 80,000 people have lost their lives due to earthquakes. The total approximate direct and indirect costs of earthquake damage between 1980 and 2022 have been calculated to be $40 billion USD [1 and 2].

Turkey has several fault lines that have the capability of generating strong earthquakes. These are the North Anatolian Fault Line (NAF) and the East Anatolian Fault Line (EAF) (Figure 1, adapted from the Turkish General Directorate of Mineral Research and Exploration, MTA [3]). The western part of the country has several fault line segments that all have the potential to generate strong earthquakes. These fault lines can all be categorized under the West Anatolian Fault Line (WAF) (Figure 1). The NAF, in the northern part of Turkey, extends close to 1,500 km, and spans east to west. In the eastern and southeastern parts of the country, the EAF extends from the Gulf of Iskenderun to the city of Hakkari, in the shape of an arc. In the western part of the country, the WAF covers an area of approximately 45,000 km^2 (almost 6% of Turkey's total land area).

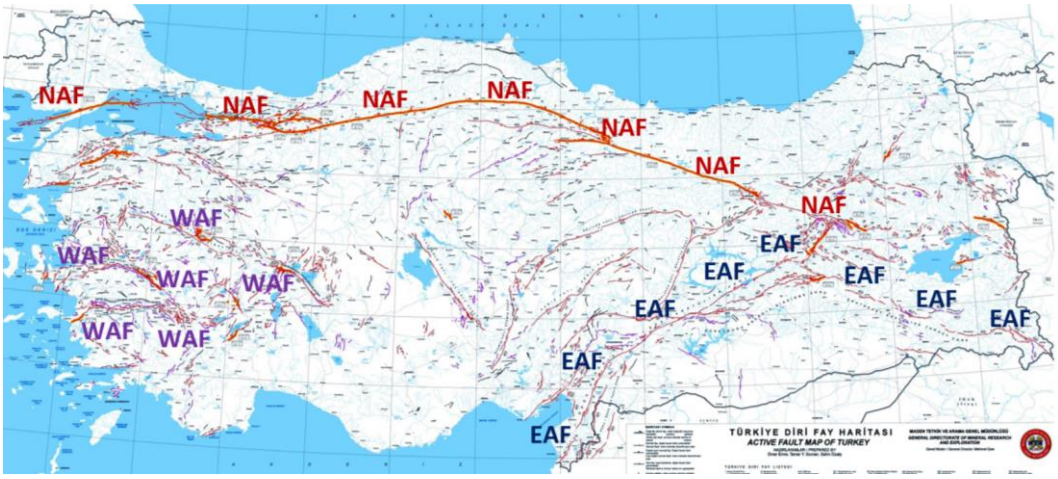

Figure 1. Turkey's active fault lines [3]

Bayraklı, İzmir, located in the western part of Turkey, suffered a strong earthquake with a magnitude of M_w = 6.6 on October 30, 2020 [4]. The hypocenter was located 16.5 km below the epicenter. The earthquake affected more than four million people, living mainly in the city of İzmir and surrounding towns and villages, as well as the residents of Samos Island, Greece. The focus of this article is on the reinforced concrete (RC) buildings located in and around İzmir; therefore, the structural damage observed in Samos are not included in this study.

İzmir is the third most populated city in Turkey, with a total of population of nearly 4.4 million people. It also has the third highest Gross Domestic Production (GDP) in the country, or 6.3% of the total GDP [5]. The city center is located approximately 67 km northeast of the epicenter of the earthquake, as shown in Figure 2. According to government data, 117 people lost their lives and close to 32,000 people were injured due to the earthquake. The earthquake caused the collapse of 11 reinforced concrete buildings immediately after the main shock. According to detailed site investigations conducted by the government, close to 6,000 buildings experienced moderate to minor damage. Out of these buildings, 511 had moderate and 5,119 had minor damage. More than 500 buildings were found to be structurally inadequate and were demolished [6].

Figure 2. Location of the Aegean Sea Earthquake (October 30, 2020)

Several scientific studies have been conducted on the 2020 Aegean Sea earthquake. While some have focused on the geotechnical and seismic aspects of the earthquake [7-10], others have concentrated on building damage [11-14]. The total direct cost of the earthquake damage was estimated to be around 400 million USD [15].

It is very important to visually record earthquake-induced damage at a site immediately after an earthquake. This can provide valuable information to experts in the field before any structural demolition and alteration take place. A reconnaissance team performed a technical visit to the earthquake-affected region within 24 hours of the earthquake. This study, which details the observations and outcomes of this site visit, adds to the current literature on the 2020 Aegean Sea earthquake by providing new on-site information regarding the seismic characteristics of the earthquake. These characteristics are based on data extracted from various strong ground motion stations, starting from the closest Turkish station near the epicenter, down to the Bayraklı District where some RC buildings collapsed and others experienced moderate to major damage. The observations and findings of this site visit, with respect to reinforced concrete buildings, are presented in this study.

2 Seismicity and Tectonics

2.1 History

During the Neotectonic Age (approx. 12 million years BC), plate movement began in the north-south direction due to the collision of the larger Arabian and smaller Anatolian plates [16] (see Figure 3). Due to the collision between the Arabian and Anatolian plates, the western part of Anatolia is moving at a speed of 40 mm/year in the counter-clockwise direction [17]. There are two large-scale important grabens (Gediz-GG and Büyükmenderes-BMG) in the region that have normal faulting mechanisms [18]. They are both young geological structures that formed in the neotectonism of Western Anatolia, and have the potential to generate destructive earthquakes. According to geological studies conducted in the region, strike-slip faulting mechanisms were also identified between these two important grabens in the N-S, NW-SE and NE-SW directions [19-21].

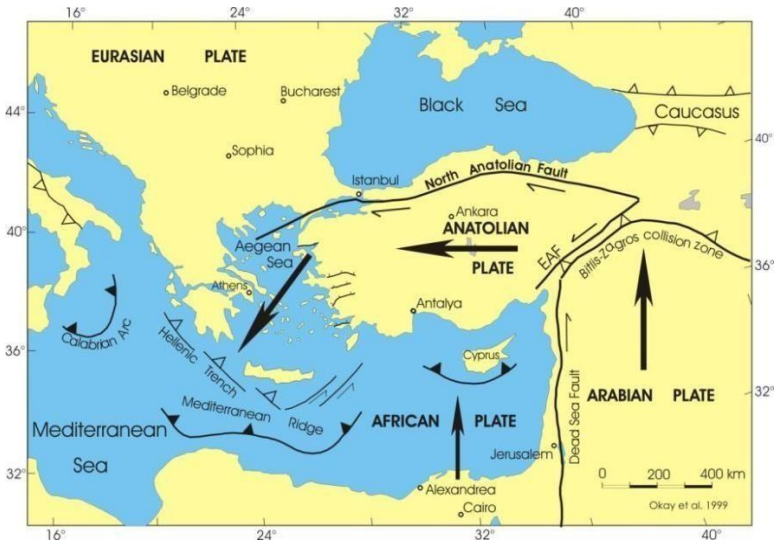

Figure 3. Intercontinental plate movement [16]

The seismicity in and around İzmir is generally governed by both normal and strike-slip fault mechanisms located between, and parallel to, the Büyük Menderes and Gediz grabens (see Figure 4). These seismic activities are predominantly controlled by the İzmir, Tuzla, Karaburun, Yenifoça, Manisa, Kemalpaşa, Seferihisar, Menemen, Gülbahçe, and Dağkızılca fault lines as well as the Gediz Graben detachment fault [22]. The İzmir and Manisa fault lines, which exist to the south and east of the İzmir Bay area, are both governed by normal faults. In the region, there are also the Tuzla and Yenifoça faults, with their strike-slip mechanisms, located in the northeast–southwest directions of the bay area [23]. The formation of İzmir Bay began through normal faults that occurred during the Early Pliocene in the western part of Turkey [24 and 25]. In the Late Quaternary, the early delta progradation of sediments emerged in the bay area [26]. Therefore, the local geology of the coastline of the İzmir Bay area consists of Quaternary alluvium surrounded by Paleocene flysch zone (limestones) and Miocene sandstones/mudstones [27-29]. The depth to bedrock in the bay area varies from 900 m to 1,200 m, while the groundwater level is between 1.0 m and 10.0 m [30 and 31].

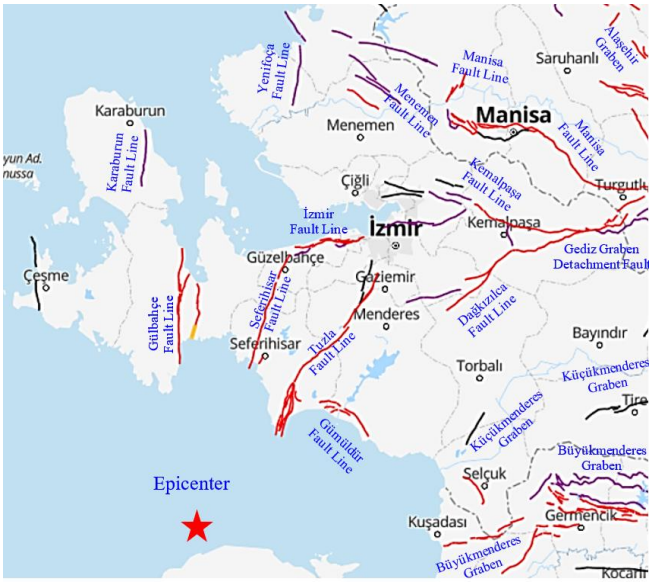

Figure 4. Active fault lines in the İzmir Area [3 and 22]

2.2 Earthquake Hazard Map

The Earthquake Hazard Map of Turkey, which was prepared based on earthquakes that have a 10% exceedance probability in 50 years, or the equivalent, to a return period of 475 years, is shown in Figure 5 [32]. Based on the peak ground accelerations illustrated in the map, the most severe earthquake regions are the northern, eastern and southeastern parts of Turkey, including the area near the Aegean Sea, the inner southwestern part of Turkey, and the area around Lake Van. Figure 6 shows a more detailed hazard map of the western part of Turkey, with expected peak ground motion acceleration values calculated based on the same return period of 475 years, along with the active fault lines [32]. Based on the data in Figure 6, the largest peak ground acceleration values in the region are around 0.4 g.

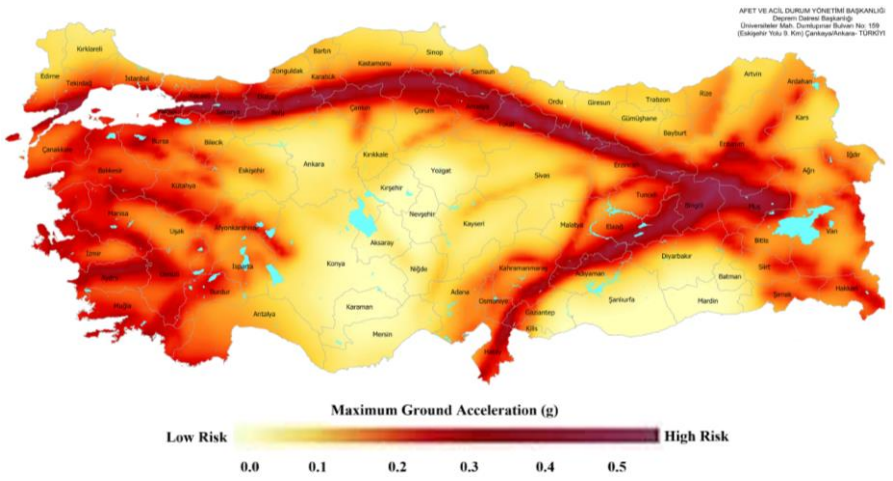

Figure 5. Earthquake Hazard Map of Turkey (return period of 475 years) [32]

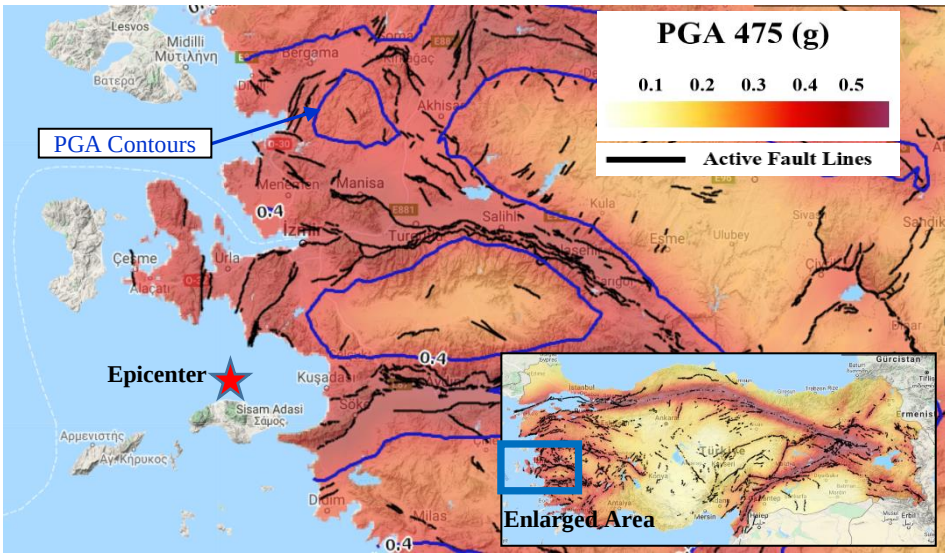

Figure 6. Expected peak ground acceleration values (in g) for earthquakes with a return period of 475 years in the western part of Turkey [32]

This article focuses on the RC buildings located in the eastern part of İzmir Bay. Therefore, it is important to emphasize the region's active fault lines and soil conditions. The map in Figure 7 shows the active fault lines and faulting mechanisms of the İzmir Bay area, including the dominant soil type [3]. Based on the map, the dominant type of soil is undifferentiated Quaternary deposits. An in-depth discussion of the soil type is provided in the next section.

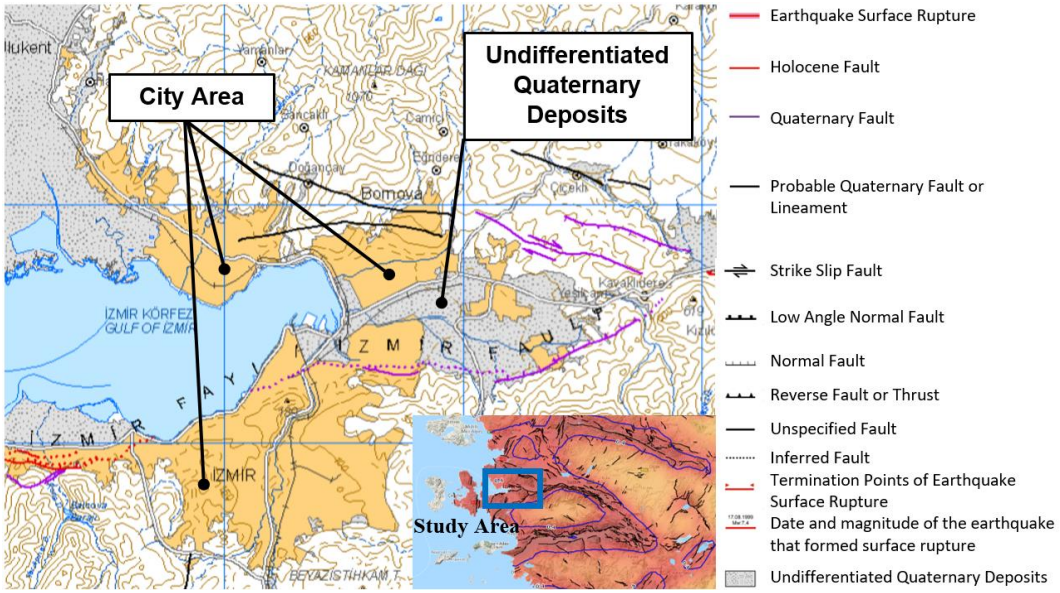

Figure 7. Active fault lines and general soil type in the İzmir Bay Area [3]

2.3 Local Soil Conditions

Figure 8-a shows the aerial view of the İzmir Bay area and the region that experienced the most severe damage, which is shaded in blue. Figure 8-b provides information related to the detailed soil types in and around the bay area. According to the map, the dominant soil type of the bay area is undifferentiated Quaternary deposits, which is a type of soil that contains siliciclastic organics and freshwater carbonates. However, the regions to the north, south and west of the study area, each at a distance of approximately 15 km away, have much better soil characteristics.

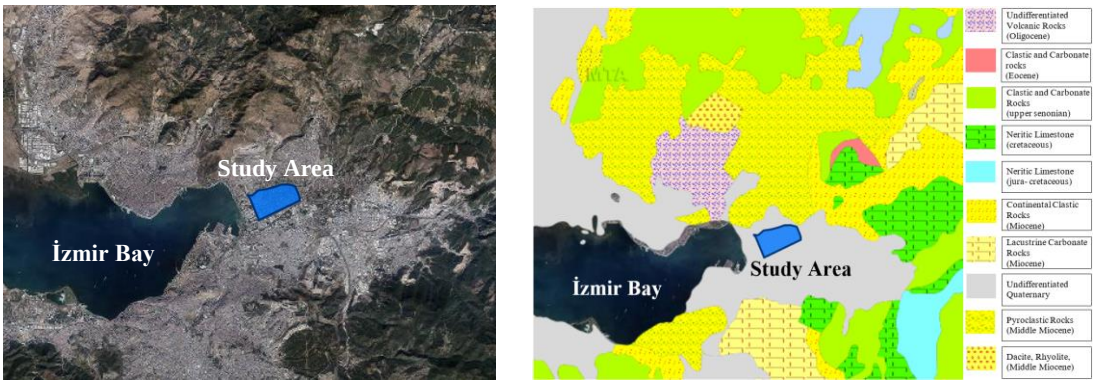

(a) (b)

Figure 8. İzmir Bay Area: (a) aerial view, and (b) soil conditions [33]

A 3D view of the study area and its soil conditions are given in Figures 9-a and b. Based on the soil conditions, it is evident that alluvial plain and delta deposits cover the entire study area and almost all the bay area [34].

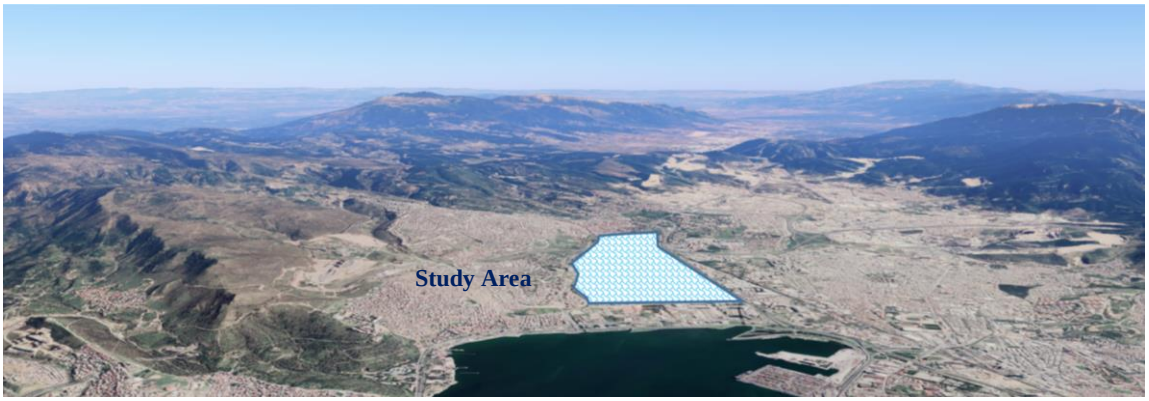

(a)

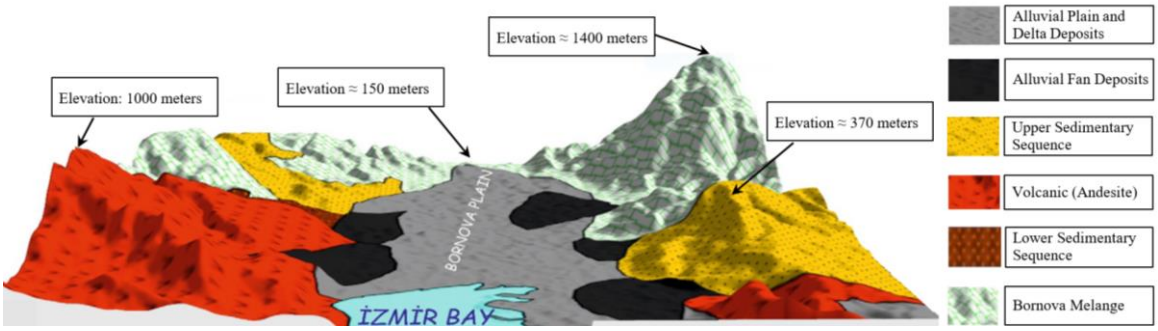

(b)

Figure 9. İzmir Bay Area: (a) 3D aerial view and (b) soil conditions [34]

2.4 The Aegean Sea Earthquake

The Aegean Sea earthquake occurred on October 30, 2020 at 14:51:23 local time [4]. The earthquake's epicenter was off the coast of Samos Island, Greece, which is located 35 kilometers away from the southwestern part of the city of İzmir. The nearest inhabited Turkish town to the epicenter is the village of Payamlı. It is located in Seferihisar, a town in İzmir Province, which was 23.4 km away from the epicenter. The earthquake had a focal depth of 16.5 km and its magnitude was measured as M_w = 6.6 [4]. Table 1 lists the time, location, magnitude and depth of the earthquake recorded by different agencies.

Table 1. Characteristics of the Aegean Sea Earthquake, October 30, 2020

Source*	Local Time	GPS Coordinates	Magnitude	Depth (km)
AFAD [4]	14:51:23	37.879 N - 26.703 E	6.6 (M_w)	16.5
KOERI [35]	14:51:26	37.902 N - 26.794 E	6.9 (M_w)	12.0
USGS [36]	14:51:27	37.918 N - 26.790 E	7.0 (M_w)	21.0
CMT [37]	14:51:35	37.760 N - 26.680 E	7.0 (M_w)	12.0
GFZ [38]	14:51:27	37.900 N - 26.820 E	7.0 (M_w)	15.0

* AFAD: Disaster and Emergency Management Authority in Turkey; KOERI: Kandilli Observatory and Earthquake Research Institute; USGS: The United States Geological Survey; CMT: The Centroid-Moment-Tensor Project; GFZ: GeoForschungsZentrum, Germany

The earthquake occurred due to normal faulting at a shallow crustal depth within the Eurasia tectonic plate of the eastern Aegean Sea. According to the USGS, the focal mechanism solution indicates that the earthquake occurred on a moderately dipping normal fault mechanism, indicating a north-south oriented extension, which is fairly common in the Aegean Sea [36]. Based on another study conducted

by the MTA, an approximately 40 km long Samos fault line ruptured during the earthquake [39]. It was also stated that the strain energy probably shifted over to the western part of the Samos fault line, extending from the North-East to the South-West. The results from the moment tensor solution of the earthquake, as prepared by different agencies, are listed in Table 2.

Table 2. Characteristic of the Aegean Sea Earthquake, October 30, 2020

Source	Moment Tensor	Strike 1	Dip 1	Rake 1	Strike 2	Dip 2	Rake 2
AFAD [4]		95	43	-87	270	46	-91
KOERI [35]		97	34	-85	272	55	-93
USGS [36]		93	61	-91	276	29	-88
CMT [37]		96	53	-86	270	37	-95
GFZ [38]		97	41	-85	272	48	-93

Historically, the İzmir region has been very active and has experienced numerous large magnitude earthquakes. Since 1900, a total of 695 earthquakes with magnitudes greater than or equal to 4.0 have been recorded during the instrumental period. Out of these 695 earthquakes, the largest magnitude was 6.8, which occurred in 1955. A total of 332 earthquakes were also recorded during the non-instrumental period, pre 1900 (Figure 10) [4 and 35].

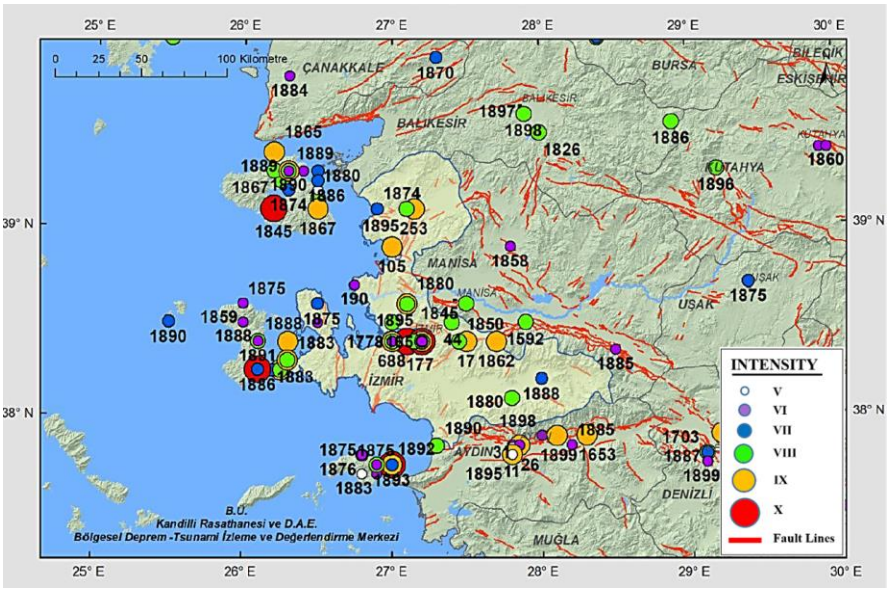

Figure 10. Pre 1900 earthquakes in and around İzmir (based on Mercalli Intensity Scale) [4 and 35]

After the mainshock of the 2020 Aegean Sea earthquake, a tsunami occurred in the region with a maximum wave height of 3.82 meters [40]. The waves in the northern direction hit the shore of the Bay of Sığacık, a district in Seferihisar, and in the southern direction, on the northern shore of Samos Island [39]. Based on the authors' site observations, the waves moved as much as 200 to 250 meters inland, into the district of Sığacık.

According to the earthquake data collected between October 30, 2020 and November 18, 2020 (20 days), a total of 4,320 aftershocks were recorded in the area, with local magnitudes varying from 0.8 to 5.2 [35]. Figure 11 shows the daily frequency distribution of these aftershock earthquakes. In order

to determine the characteristics of the aftershocks, the total number of aftershocks is also categorized according to their magnitudes, as displayed in the figure.

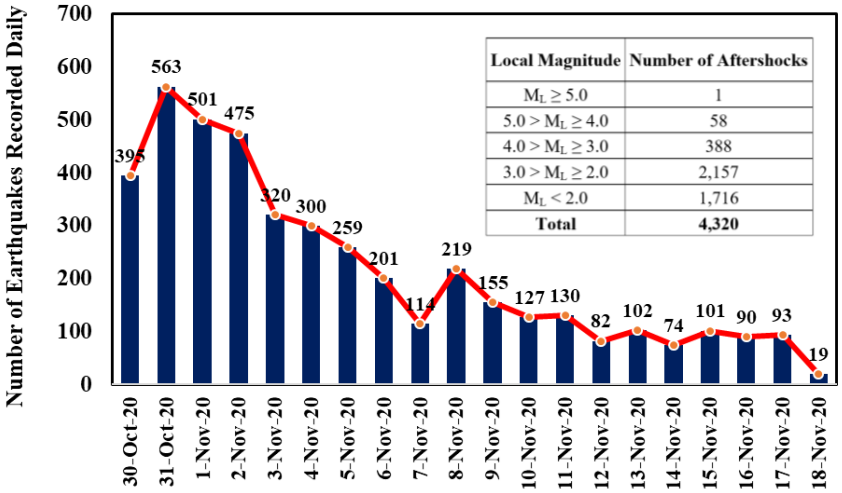

Figure 11. Total number of aftershocks recorded in the region between October 30, 2020 and November 18, 2020

Table 3 shows the peak ground acceleration values that were recorded by AFAD at the nearest sixteen strong ground motion stations [32]. The locations of these stations are plotted on the map in Figure 12. The closest station to the earthquake was the Seferihisar station (station number 3536), which was 35 kilometers away from the epicenter. The most distant one was the Bornova station (station number 3520), which was 76 kilometers away from the epicenter. The maximum peak ground acceleration recorded at the Kuşadası station (station number 0905) was in the East direction with a magnitude of 0.179 g.

Table 3. Earthquake data extracted from the 16 strong ground motion recording stations

No	Station Number	City	Town	Latitude (°)	Longitude (°)	Peak Ground Acceleration Values (gal)			R_{epi} (km)
						NS	EW	Vertical	
1	3536	İzmir	Seferihisar	38.1968	26.8384	50.220	79.139	31.315	34.745
2	0905	Aydın	Kuşadası	37.8560	27.2650	179.314	144.017	79.839	42.948
3	3523	İzmir	Urla	38.3282	26.7706	80.320	63.572	36.899	48.940
4	3533	İzmir	Menderes	38.2572	27.1302	73.635	45.899	37.460	51.380
5	3516	İzmir	Güzelbahçe	38.3706	26.8907	47.291	48.356	32.082	54.565
6	3538	İzmir	Gaziemir	38.3187	27.1234	85.484	76.953	39.264	56.665
7	3506	İzmir	Konak-1	38.3944	27.0821	43.879	41.039	23.587	62.304
8	3517	İzmir	Buca-1	38.3756	27.1936	40.099	36.136	19.816	65.316
9	3512	İzmir	Buca-2	38.4009	27.1516	57.541	56.746	28.158	65.761
10	3518	İzmir	Konak-2	38.4312	27.1435	106.103	91.449	31.143	68.365
11	3519	İzmir	Karşıyaka-1	38.4525	27.1112	150.089	109.975	34.173	69.225
12	3521	İzmir	Karşıyaka-2	38.4679	27.0764	110.844	93.986	40.312	69.581
13	3522	İzmir	Bornova-1	38.4357	27.1987	73.721	63.941	24.647	71.182
14	3513	İzmir	Bayraklı-1	38.4584	27.1671	106.281	94.667	44.186	72.002
15	3514	İzmir	Bayraklı-2	38.4762	27.1581	39.421	56.024	25.148	73.388
16	3520	İzmir	Bornova-2	38.4780	27.2111	36.112	58.549	19.367	75.777

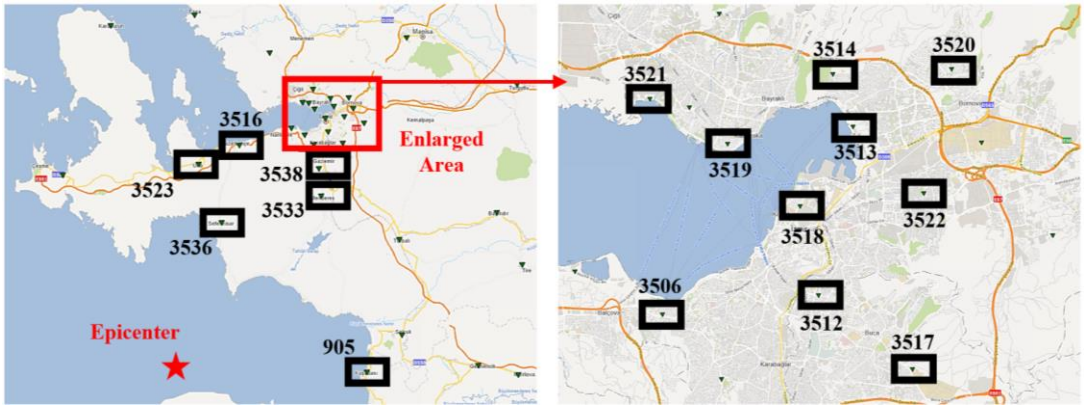

Figure 12. The locations of the 16 strong ground motion recording stations

2.5 Arias and Housner Intensities and Spectral Acceleration Values of the Aegean Sea Earthquake

Figure 13-a illustrates the variation of the horizontal and vertical peak ground accelerations from the nearest station (Seferihisar, station number 3536) to the farthest one (Bornova, station number 3520). The figure shows a total of three peaks at the epicentral distances of 40 km (Kuşadası, station number 0905), 55 km (Urla and Güzelbahçe, station numbers 3523 and 3516) and 70 km (İzmir Bay area, including Bayraklı and Karşıyaka, station numbers 3513 and 3519), which were all associated with local site conditions. The acceleration peak at the epicentral distance of 70 km is a lot more pronounced than the other two peaks. This led to the immediate collapse of eleven buildings and severe structural damage in the Bayraklı district. Figure 13-b illustrates the variation of the earthquake's effective time. Based on the data, the effective time increased as the earthquake moved into the İzmir Bay area, leading to an increase from an average of 16 seconds to 23 seconds in the horizontal directions. This increase was more prominent in the vertical component of the earthquake.

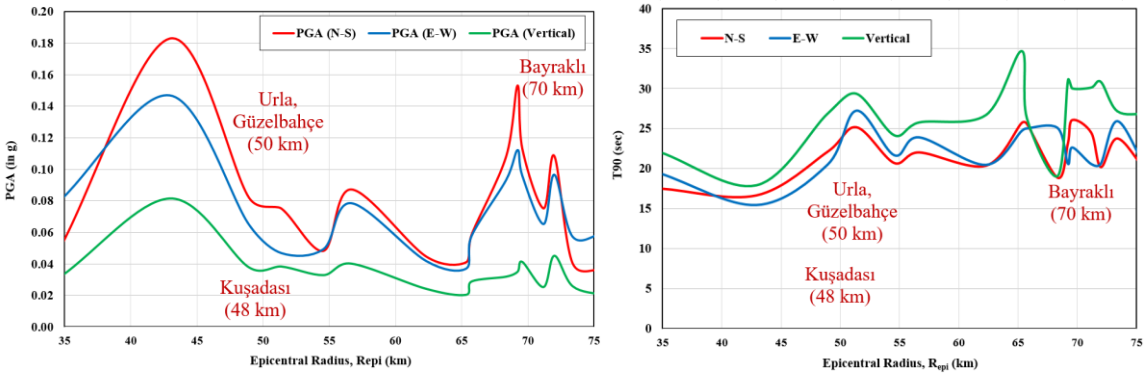

(a) (b)

Figure 13. The Aegean Sea Earthquake: (a) PGA, and (b) effective time duration

The variations of the Arias and the Housner Intensities of the Aegean Sea earthquake are plotted in Figure 14-a and b in the N-S, E-W and vertical directions based on the ground motion data recorded at 16 stations (see Figure 12 for their locations). Based on the data used in these figures, it is clear that the intensity of the earthquake was greater in the regions around İzmir Bay, Bayraklı and Karşıyaka.

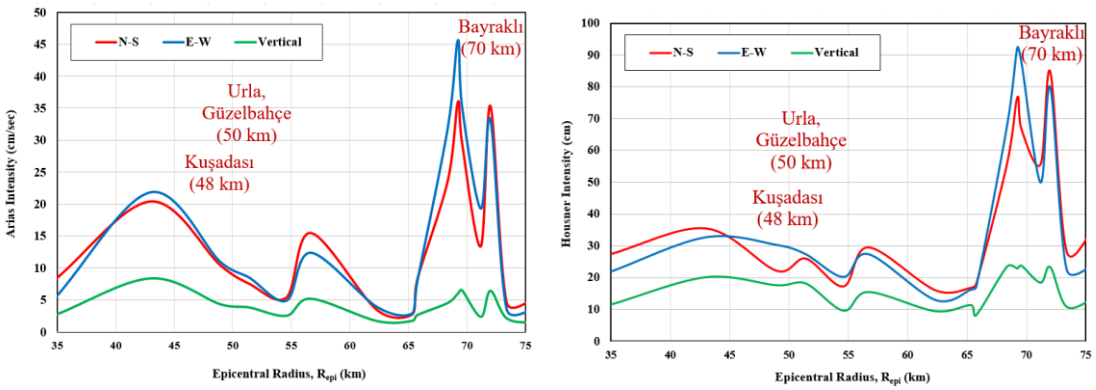

(a) (b)

Figure 14. The Aegean Sea Earthquake: (a) Arias intensity and (b) Housner intensity

3 Evaluation of Strong Ground Motion Data

The strong ground motion data is evaluated at six stations to better understand the impact and characteristics of the earthquake, specifically in the bay area (see Figure 15). These stations are located along the earthquake route, starting from Kuşadası (station number 0905) to the station in the most affected area, Bayraklı (station number 3513), in the following order: 0905, 3536, 3518, 3513, 3519 and 3514. However, emphasis is given to the results extracted from the following three stations in and around the town of Bayraklı, which encircles the İzmir Bay area: 3513, 3518 and 3519.

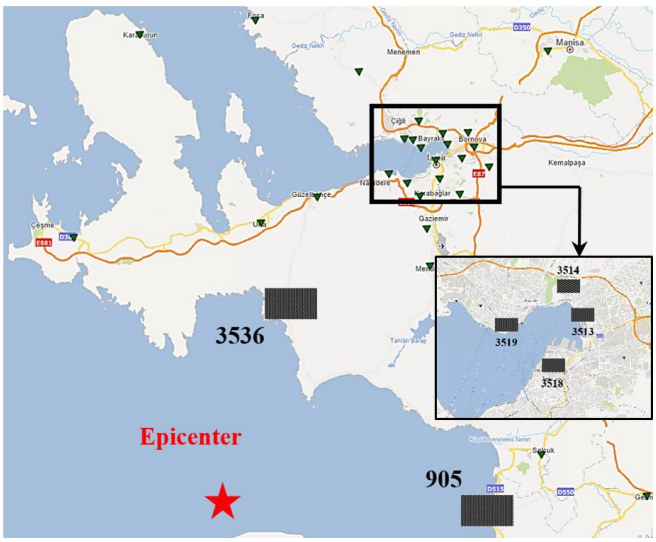

Figure 15. Locations of the six strong ground motion stations used to evaluate the Aegean Sea Earthquake data

Figure 16 illustrates the peak ground acceleration values of the Aegean Sea earthquake in the North-South and East-West directions recorded at the six stations. According to the data, the largest peak ground acceleration values were recorded at station number 0905 (located in the town of Kuşadası). The values at this station in both directions were 0.18 g and 0.15 g, respectively. The acceleration values are also provided in the Bayraklı area, where building collapses and severe structural damage were observed. The nearest station to Bayraklı is number 3513; it recorded 0.11 g and 0.10 g peak ground accelerations in the North-South and East-West directions, respectively.

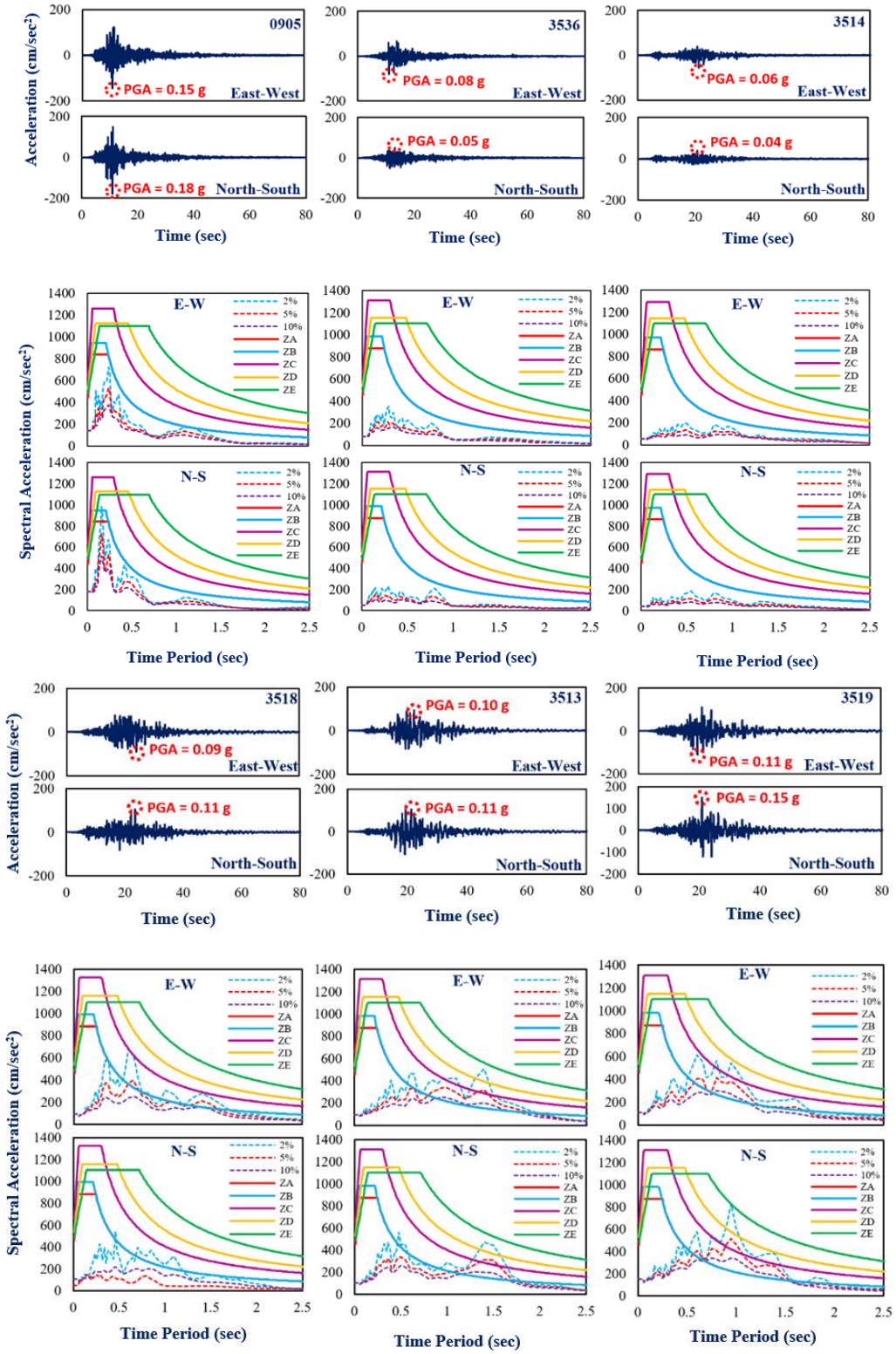

Figure 16. Peak ground and spectral acceleration values and design spectrum values for the Aegean Sea Earthquake, October 30, 2020

The design spectrum curves of the current Turkish Building Earthquake Code (TBEC, 2018) [41] were compared to the measured spectral acceleration data, which were extracted from the six stations in the North-South and East-West directions as a function of varying damping ratios (see Figure 16). TBEC (2018) [41] defines a total of 6 local soil classes, identified by letters ZA through ZF, where ZA defines a soil type of hard rock, and ZF defines a soil type of extremely loose soil, which needs further soil testing and site evaluation. In this study, the design spectrum curves of the first 5 soil classes (excluding soil type ZF) were used to evaluate the North-South and East-West peak ground acceleration components of the Aegean Sea earthquake. Based on the spectrum values, the peak ground acceleration values at station numbers 3536 and 3514 were much less than the demands associated with the 5 soil classes. Therefore, the structural damage at these locations were moderate to minor. However, as the seismic waves travelled along station numbers 0905, 3518, 3513 and 3519, their corresponding periods for the peak ground accelerations shifted from 0.2 to 1.5 seconds. This shift exceeded the code generated design response spectrum values, specifically at station numbers 3513 and 3519, for all four soil types, except type ZE. As a result of this exceedance, the degree of structural damage varied from moderate to intense in RC buildings with 8 to 15 floors.

In order to further evaluate the impact of the Aegean Sea earthquake, the local soil classes of the selected stations were taken into account. Figure 17 shows the soil classes at these stations [42]. Based on this data, the soil properties of the İzmir Bay area are found to be the weakest since almost all the stations are located in soil classes ZD or ZE, which confirms the soil properties explained in Section 2.3. As expected, the weak soil amplified the peak ground acceleration and extended the effective time duration by causing building collapses and severe structural damage. Although station numbers 3518 and 3519 both displayed a very similar acceleration pattern to station number 3513, the building damage near these two stations were not as severe as those at 3513. The severe building damage near station number 3513 are largely attributed to the regions' local soil type (alluvial plain and delta deposits) (see Figure 8-b). The other reason for this problem is the lack of geotechnical studies, which were not mandated at the time of construction (for further information see Section 4.5.5).

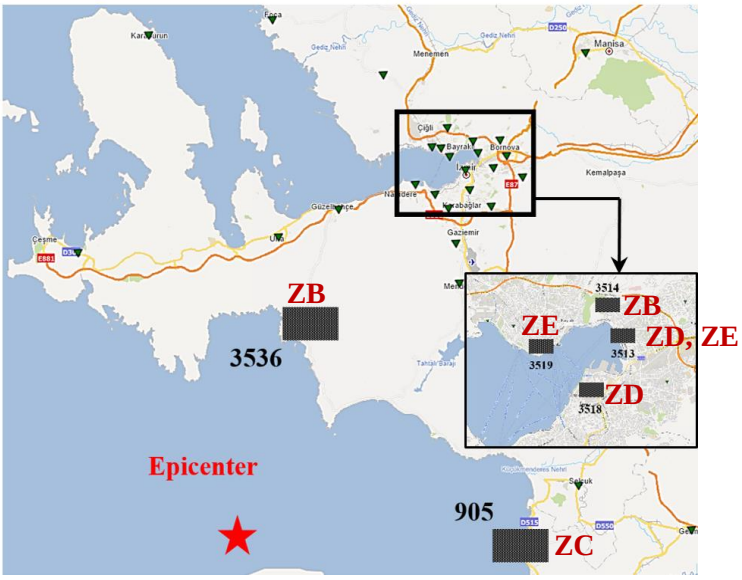

Figure 17. Local soil classes for the selected six stations

4 Earthquake Performance of Reinforced Concrete Buildings

The technical team visited the earthquake-affected locations 10 hours after the earthquake to avoid missing any data related to the condition of the buildings during the search and rescue operations. Detailed observations and investigations were performed at the collapsed, partially collapsed, and damaged building sites during the four-day stay of the technical team.

Damage Assessment Yazısı referansları ile birlikte buraya girilecek (gtunc)

The findings and evaluations explained in this section are the result of the data and evidence collected during the numerous visits to the related sites at various times. First, the overall impact of the earthquake will be explained, then the findings of the site visits will be discussed to identify the reasons behind structural damage. With the exception of the images from Google Maps, all of the photographs featured in this section were taken by (and are the property of) the authors.

4.1 Building Inventory and Damage Statistics in Izmir

In January 2019, the total number of buildings in Izmir was 830,447 [43]. Based on data provided by the Turkish Statistical Institute, almost 70% of the buildings in İzmir are reinforced concrete; the remaining are masonry [14]. Residential buildings constitute approximately 90% of all buildings. Figure 18 illustrates the distribution of RC buildings in İzmir.

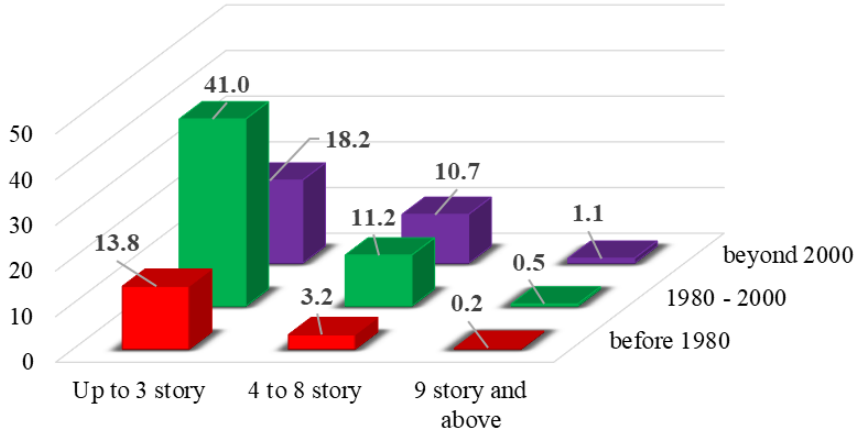

Figure 18. Distribution of RC buildings in İzmir by percent (adapted from [14])

As illustrated in Figure 18, 73% of the RC buildings have up to 3 floors, 25% of them have 4 to 8 floors, and the remaining (almost 2%) have 9 floors and above. As a group, 70% of these RC buildings were built before 2000. There were mainly two earthquake codes in effect at the time, the 1975 and 1998 earthquake codes. Based on the number of years and buildings constructed, it is accurate to state that out of 70% of the buildings, almost 60% of them were built according to the rules and regulations of the 1975 Turkish earthquake code.

Only a few government-approved institutions were allowed to investigate the buildings (RC and masonry) at the earthquake site. Table 4 lists the findings of one of these institutions [14 and 44].

According to the data, 0.81% of the buildings experienced moderate to major level of damage, while 4.23% of the buildings experienced minor damage. The total number of buildings with no damage constituted 95% of the total building inventory. As discussed in Section 4.2, the buildings with major damage and those that collapsed and demolished were all from the Bayraklı District.

Table 4. October 20, 2020 dated damage assessment of the buildings in İzmir after the 2020 Aegean Sea earthquake (adapted from [14])

	Collapsed	Demolished	Major Damage	Moderate Damage	Minor Damage	No Damage	Total
Number of Buildings	50	35	581	688	6,683	150,084	158,121
Percentage of Total	0.03	0.02	0.37	0.44	4.23	94.92	100.00

The distribution of the damage levels of the RC buildings in İzmir is also plotted in Figure 19, as a function of their construction years. As the data indicates, most of the moderate to major size damage was observed in buildings constructed between 1990 and 2000. Beyond 2010, it was observed that the damage level shifted towards minor level damage.

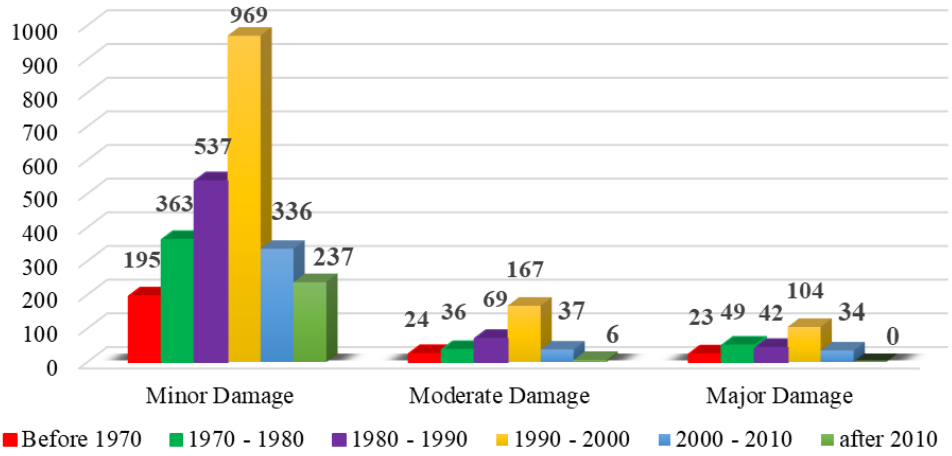

Figure 19. Distribution of damage in İzmir's RC buildings by numbers (adapted from [14])

4.2 Collapsed Buildings

As stated in Section 1, the earthquake caused the sudden collapse of 11 RC buildings. Out of these 11 RC buildings, 4 of them (Rıza Bey, Doğanlar, Emrah, and Block B of Yağcıoğlu Apartment Complex) completely collapsed and 7 of them (Yılmaz Erbek and Karagül Apartments, three blocks in the Barış Apartment Complex and two blocks in the Cumhuriyet Apartment Complex) partially collapsed in the Bayraklı District during the earthquake. All the collapsed buildings had structural framing systems consisted of reinforced concrete columns and beams. These frames were infilled using brick masonry at all the story levels except the ground story. Most of them had shops at the ground story which may have produced weak story at the ground floor levels. General information related to the collapsed buildings is shown in Table 5. The locations of these buildings are shown in Figure 20.

Table 5. General information related to collapsed buildings

Name of Apartment	Number of Stories	Start of Construction	End of Construction	Usage	Collapse Type
Rıza Bey	9	1993	1994	32 flats and 5 shops	Completely
Doğanlar	8	1990	1992	21 flats and 4 shops	Completely
Emrah	8	1990	1993	28 flats and 6 shops	Completely
Yağcıoğlu Sitesi (2 Blocks)	8	1993	-*	14 flats and 4 shops in each block	Block B Completely
Yılmaz Erbek	10	Ends of 1990s	-*	2 shops	Partially (half of the building)
Karagül	8	1990s	-*	28 flats	Partially (quarter of the building)
Barış Sitesi (4 Blocks)	8	1992	-*	-*	Partially (3 Blocks)
Cumhuriyet Sitesi (3 Blocks)	8	1990s	-*	-*	Partially (2 Blocks)

* Information could not be obtained.

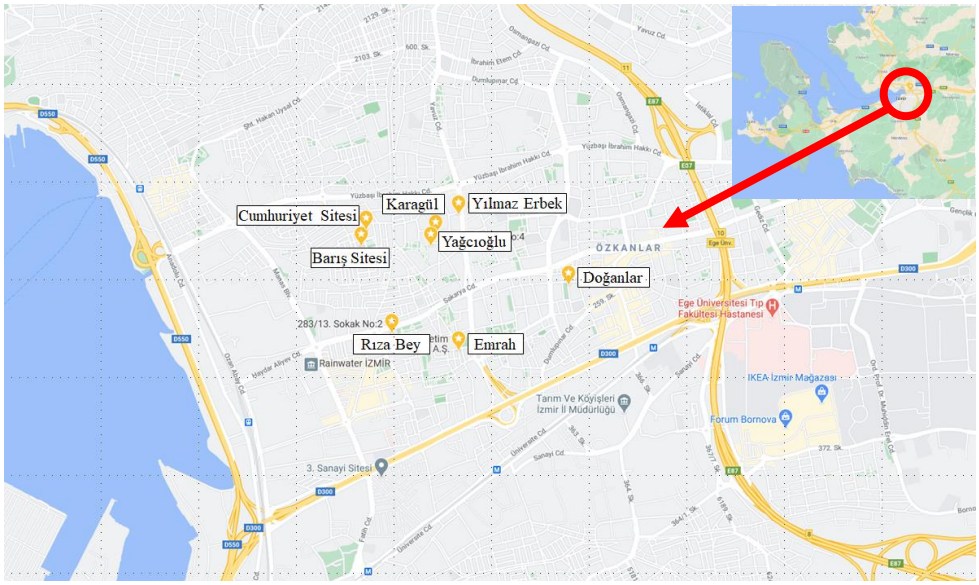

Figure 20. Locations of collapsed buildings in the Bayraklı District

A nine-story building, the Rıza Bey Apartment, collapsed fully during the earthquake. The construction of the building was completed in 1994. The building consisted of 32 separate apartments and 5 shops at the ground-story level. The collapse of this building started with the failure of ground story columns based on the videos shot during the collapse. After the rest of the building shifted one story down, all the other stories started to collapse progressively one by one, one on top of each other, without any translation in the horizontal direction. Photographs of the building before and after the earthquake are shown in Figure 21.

Figure 21. Photographs of the Rıza Bey Apartment Building before and after the earthquake

The Doğanlar Apartment Building, with its 21 apartments and 4 shops at the entrance level, collapsed approximately 1 minute after the earthquake. The construction of this 8-story building was finished in 1992. One side of this building was adjacent to another building, with a small gap in between. During its collapse, the Doğanlar Apartment Building shifted away from the adjacent building. Photographs of the building before and after the earthquake are shown in Figure 22.

Figure 22. Photographs of the Doğanlar Apartment Building before and after the earthquake

Another collapsed building was the 8-story Emrah Apartment Building, completed in 1993. The apartment housed 6 shops on its ground floor and 28 separate apartments above it. Photographs of the building before and after the earthquake are shown in Figure 23.

Figure 23. Photographs of the Emrah Apartment Building before and after the earthquake

Block B of the Yağcıoğlu Apartment Complex collapsed fully after the earthquake, whereas Block A survived the earthquake with heavy damage. Each block of this apartment complex consisted of an 8 story building with 14 separate apartments and 4 shops, located at the ground level. Both buildings

were constructed in 1993. Photographs of the buildings before and after the earthquake are shown in Figure 24.

Figure 24. Photographs of Block B of the Yağcıoğlu Apartment Complex before and after the earthquake

The Yılmaz Erbek Apartment Complex consisted of two adjacent 10-story blocks. This building was constructed in the late 1990s. The ground story level consisted of shops, and the rest of the stories were comprised of separate apartments. The first two stories of one of the blocks collapsed during the earthquake. The partially-collapsed building separated from the other building and the total height was reduced. Photographs of the building before and after the earthquake are shown in Figure 25.

Figure 25. Photographs of the Yılmaz Erbek Apartment Complex before and after the earthquake

The 8-story Karagül Apartment Building, with 28 separate apartments and shops at the ground level, was heavily damaged during the earthquake. This building was constructed in the early 1990s. Each residential story consisted of four apartments and only one fourth of the building area (corresponding to one apartment) collapsed partially a few minutes after the earthquake. Photographs of the building before and after the earthquake are shown in Figure 26.

Figure 26. Photographs of the Karagül Apartment Building before and after the earthquake

The Barış Apartment Complex, which was comprised of four blocks with 8 stories each, was constructed in 1992. Three of these buildings partially collapsed and one of them experienced extensive damage without collapse. The first four stories of the two blocks and the first three stories of the other block collapsed on top of each other. The stories over the collapsed portion of the buildings survived the earthquake by leaning towards one side of the buildings. Photographs of the Barış Apartment Complex before and after the earthquake are shown in Figure 27.

Figure 27. Photographs of the Barış Apartment Complex before and after the earthquake

A similar failure mode was observed in the Cumhuriyet Apartment Complex constructed in the early 1990s. The complex consisted of 3 blocks with 8 stories each. One block survived the earthquake with heavy damage; however, the first story of the other two blocks collapsed, causing the uncollapsed section of the buildings to shift one story down. Photographs of the Cumhuriyet Apartment Complex before and after the earthquake are shown in Figure 28.

Figure 28. Photographs of the Cumhuriyet Apartment Complex before and after the earthquake

4.3 Severely Damaged Buildings

There were numerous severely damaged buildings in the city of İzmir during the Aegean Sea earthquake. One of the typical damage types was diagonal cracking on structural (beams, columns, and shear walls) and non-structural (partition walls) elements, as shown in Figure 29. The structural damage on the columns were also very significant in some of the buildings, as shown in Figure 30. On the other hand, some of the buildings constructed side by side were separated due to the collision (hammering effect) of these buildings moving in opposite directions during the earthquake. This type of motion results in the damage of the structural elements of these buildings. An example of this behavior is shown in Figure 31.

Figure 29. Diagonal cracks on structural and non-structural elements

Figure 30. Severe column damage

Figure 31. Separated buildings constructed side by side

4.4 Evolution of Earthquake Codes in Turkey

The first Turkish Earthquake Code, TEC (1940), [45], was published in 1940, and was originally adapted from the Italian Earthquake Code that was valid at the time. This code was modified nine times, to date. The last four of versions pertain to this study, and were published in 1975 [46], 1998 [47], 2007 [48], and 2018 [41].

The partially and fully collapsed reinforced concrete buildings in this earthquake were constructed in the 1990s (between 1990 and 1998) when TEC (1975) [46] was in effect. TEC (1975) [46] was considered successful when it was prepared. According to TEC (1975) [46] the earthquake loads on buildings were calculated by multiplying an earthquake load coefficient by the seismic weight (calculated using the self-weight and a portion of live loads) of the building. Factors such as earthquake zones (4 zones), building importance factors (2 factors), soil types (12 types), the fundamental period of the building, design acceleration spectrums (4 types), and the ductility levels of

the building (2 types) were used to determine this coefficient. Based on this code, the calculated base shear for residential buildings was approximately 8% to 15% of the seismic weight of the building. The equivalent lateral static force procedure was used to distribute the total base shear to the story levels. No minimum concrete compressive strength was defined for residential buildings in this code; however, a minimum concrete compressive strength of 22.5 MPa was specified for buildings located in 1st and 2nd earthquake zones with an importance factor of more than one. There was no provision related to the type (plain or deformed bars) and minimum yield strength of reinforcing steel bars. It was very well known that the largest sectional forces would develop at the beam and column ends. Therefore, the provisions related to the confinement of the beam and column ends and the bending stirrups ends into the concrete core (135° hooks) were also included in TEC (1975) [46]. Additionally, provisions related to short columns were incorporated into this specification.

Starting with TEC (1998) [47], the strong beam-stronger column methodology was introduced into the design of reinforced concrete buildings in Turkey. This required that the resisting moment capacities of the connecting columns of a joint be greater (minimum 20% or more) than that of the connecting beams of the same joint in the same plane. When the building is subjected to earthquake forces, damage (plastic hinging) will first form at the bottom ends of the first story columns. Consequently, plastic hinges will always form at the beam ends, if a building is constructed based on the strong beam-stronger column criterion. The collapse of the building will require the formation of hinges at both beam ends, resulting in the highest possible energy absorption capacity before failure. This criterion was also followed in later codes.

Other provisions of TEC (1975) [46] such as confinement of concrete at beam and column ends and bending of stirrups were explained in more details in TEC (1998) [47], TEC (2007) [48], and Turkish Building Earthquake Code [41]. The calculated base shear for residential buildings was approximately 12.5% to 25% percent of the seismic weight of the building for these three later codes. A comparison of the last four Turkish earthquake codes for RC buildings is shown in Table 6.

Table 6. A Comparison of the last four Turkish Earthquake Codes for RC buildings.

Description	Turkish Earthquake Codes			
	1975 [46]	1998 [47]	2007 [48]	2018 [41]
Minimum Concrete Strength (MPa)	No limit*-22.5**	16*-20***	20*	25*
Minimum Yield Strength of Steel (MPa)	Not Specified	Not Specified	Not Specified	420 or Greater
Allowed Reinforcement Bar Type	Plain	Plain/Deformed	Deformed	Deformed Only
135° Stirrup Hooks	Yes	Yes	Yes	Yes
Confinement Region at Ends of Beams	Yes	Yes	Yes	Yes
Confinement Region at Ends of Columns	Yes	Yes	Yes	Yes
Strong Beams, Stronger Columns	No	Yes	Yes	Yes

* For all buildings in all earthquake regions

** Buildings located in the first and second earthquake regions with an importance factor of more than one

*** Buildings located in the first and second earthquake regions with an importance factor of more than one or ductile behavior

4.5. Evaluation of Collapsed and Severely Damaged Buildings

All the fully and partially collapsed buildings in this study were designed and constructed before the TEC (1998) [47] was in effect. Therefore, the provisions of the TEC (1975) [46] will be used to evaluate the design, construction, and behavior of these buildings during this earthquake.

Some of the collapsed or severely damaged buildings were structurally evaluated for their risk of collapse during an earthquake in recent years (between 2012 and 2018). Corresponding Structural Evaluation Reports (SER hereafter) [49 and 50] were prepared and submitted to the inhabitants of these buildings long before the 2020 Aegean Sea earthquake. The information in these SER [49 and 50] was also used to evaluate the behavior of the buildings in this section.

Summary of the problems resulting in damage and collapses is shown in Figure 32. It is important to note that these problems are not just common to RC buildings in Turkey but are also common to other types of buildings, such as masonry and timber ones, resulting from the past earthquakes that occurred in the region and around the world [55, 56 and 57]. Details of these problems are explained in the following sub-sections.

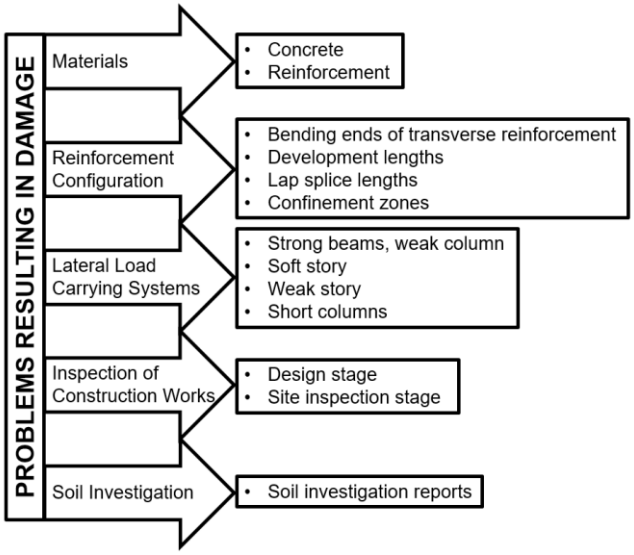

Figure 32. Summary of the problems resulting in damage

4.5.1. Problems Related to Materials

No minimum concrete compressive strength was specified in TEC (1975) [46] for the residential buildings that collapsed during this earthquake. According to the SER, a concrete compressive strength ranging from 10 to 17 MPa was used in the construction of these buildings [49 and 50]. These values were determined using ultrasonic and surface hardness tests performed on these buildings. However, one should adopt these results with caution since non-destructive testing of concrete compressive strength is unreliable and should be used in combination with the traditional coring technique. The concrete compressive strengths obtained from these tests were lower than those specified in the structural drawings of these buildings.

Based on site observations of the concrete members of the collapsed buildings, it was determined that the concrete used in these buildings consisted of round coarse aggregates, 30 to 50 mm in diameter.

Round and large sized aggregate would result in poor interlocking behavior and weak bond strength between concrete and steel reinforcement. Photographs of some of the concrete samples are shown in Figure 33.

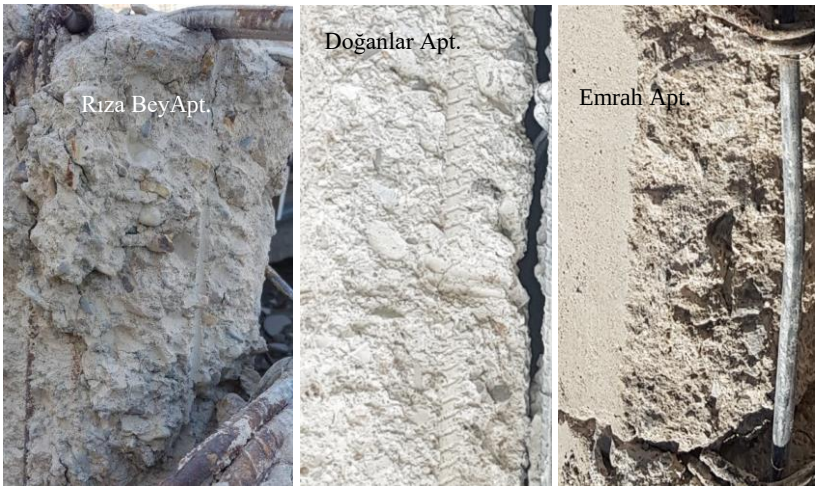

Figure 33. Concrete quality in various collapsed buildings

TEC (1975) [46] did not specify the type of steel reinforcement that should be used in reinforced concrete buildings. Only plain longitudinal and transverse reinforcing bars were available in the early 1990s in Turkey. These steel reinforcing bars had a minimum yield strength of 220 MPa. Deformed reinforcing bars became available towards the mid-1990s. Visual observation of the collapsed buildings confirmed that combinations of these reinforcements were used during the construction of these buildings. For example, plain bars were used in the construction of the Emrah Apartment, both as longitudinal and transverse reinforcements. The longitudinal and transverse reinforcements used in the Rıza Bey Apartment were deformed and plain, respectively. In the Yılmaz Erbek Apartment, only deformed bars were used as reinforcement. Photographs of these reinforcements are shown in Figure 34.

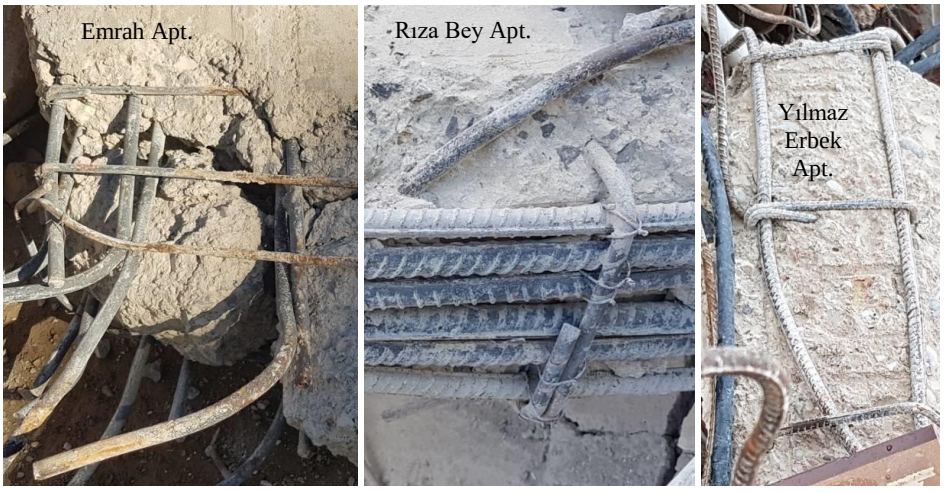

Figure 34. Reinforcement types in various collapsed buildings

Most of the buildings in the area had moisture problems due to the humid climate, the high water table level, and insufficient water insulation, especially at the ground floor level. Therefore, the reinforcements of the structural members of these buildings corroded extensively, resulting in significant reduction of the cross-sectional area of the reinforcements. Examples of corroded reinforcements are shown in Figure 35. It is important to note that these mistakes are repeating themselves when building damage is investigated in most earthquakes. For instance, the field observations recorded after the Sivrice, Elazığ, Turkey earthquake on January 24, 2020, are an example of this [51].

Figure 35. Corrosion of reinforcements due to moisture

4.5.2. Problems Related to Reinforcement Configuration

As stated above, TEC (1975) [46] required closely spaced stirrups (confinements) to be used at the end regions (confinement zones) of beams and columns. The length of this region was a minimum of one-sixth of the column height, or 450 mm for columns. TEC (1975) [46] also specified the distance between the two stirrups in this region as a maximum of 100 mm. The site observations indicated that no confinement was used at the ends of beams and columns. Examples of the reinforcement configurations of the columns and beams of the collapsed buildings are shown in Figure 36. This finding was also supported in the various SER [49 and 50] prepared for these collapsed buildings.

Figure 36. Reinforcement configurations of the columns and beams of the collapsed buildings

Although TEC (1975) [46] required bending the ends of the stirrups into the concrete core (135° hooks), the ends of the stirrups were only bent 90°, resulting in the opening of the stirrups after the spalling of the cover concrete in the beams and columns. Photographs of these stirrups in various collapsed buildings are shown in Figure 37. As with the observation made in the materials section, the issues related to reinforcement configuration are another problem that has been frequently observed in Turkey following an earthquake.

Figure 37. Ends of the stirrups (bent 90°) of the collapsed buildings

4.5.3. Problems Related to the Lateral Load Carrying Systems

TEC (1975) [46] did not define any irregularity based on story stiffness. The effect of this type of irregularity was first introduced into the earthquake code in 1998 [47]. The strong beam-stronger column requirement also first appeared in TEC (1998) [47]. The first few stories of some of the buildings collapsed like a sandwich during the earthquake. These buildings had story stiffness irregularities at the ground story level which probably played a major role in the collapse. Photographs of these buildings are shown in Figure 38.

Figure 38. Collapsed buildings due to the failure of first story columns

According to TEC (1975) [46], the confinement of transverse reinforcement was applied along the length of the short columns. An example of damage due to short columns after this earthquake is shown in Figure 39. No confinement of reinforcement was observed along the short columns.

Figure 39. Short column formation in a severely damaged building

4.5.4. Problems Related to Inspection of Construction Works

Before the beginning of millennium, the inspection of construction works in Turkey was not properly performed. Reports related to soil investigations and structural designs were not reviewed by any institution. During construction, the strength of materials (concrete and steel) used were not tested, and the correct application of the structural drawings in terms of reinforcement configuration and dimensions of structural members were not confirmed. In some of the collapsed and severely damaged buildings, the SER prepared before the earthquake indicated that the reinforcement configuration of the structural drawings was different than that found in the constructed buildings. Furthermore, the sizes of the constructed structural members did not match those in the structural drawings of some of the buildings [49 and 50]. For example, a column that was 250×800 mm in size in the structural drawings was, in 1988, constructed as 250×500 mm in size, along the height of a 9-story building.

The inspection mechanism before (the design stage) and during the construction process changed significantly in the 2000s. After the earthquake, the conditions of numerous damaged buildings in İzmir were investigated by experts from the Turkish Ministry of the Environment and Urbanization. Based on their findings, some of the buildings were determined to be unsafe for occupants, and were either demolished immediately, or designated to be repaired and/or strengthened. During this post-earthquake assessment process, it was observed that the structural members of some of the buildings were damaged or destroyed for various reasons, before the earthquake. Examples of this type of damage and destruction are shown in Figure 40. The bottom longitudinal reinforcement of the basement beam shown in this figure was cut at the midspan, and the top longitudinal reinforcement was damaged at the support region in order to install utility pipes inside the building. The stirrups at the damaged sections were also cut.

Figure 40. Beam damaged due to plumbing (Karşıyaka, İzmir)

4.5.5 Problems Related to Soil Investigation

In Turkey, early geotechnical site studies were initiated as part of a requirement in zoning plans in 1986 [51]. However, it was not until two major earthquakes occurred—the Kocaeli Earthquake of August 1999, and the Düzce Earthquake of November 1999—that the existing law was amended to

require geological site reports as part of the building permit acquisition process [52]. Since there were issues regarding the content of geotechnical reports, the government intervened and furnished the details of a typical site report. As part of these efforts, in January 2000, the Ministry of Public Works issued a memorandum making geotechnical site reports a structural design requirement. As the historical evolution of geotechnical site reports in Turkey suggests, soil-associated structural design parameters were not a priority until the early 2000s. This issue clearly underscores the problem in buildings constructed before 2000. Most likely, this issue played a significant role in the buildings that collapsed and experienced moderate-to-major damage in the Bayraklı District [53 and 54].

5 Conclusions

The following conclusions can be drawn based on the technical team's site observations:

- The local soil class (site effect) is an important parameter to be incorporated into the earthquake analysis and design of a building. The buildings in Bayraklı suffered mostly from this phenomenon. Therefore, it is recommended that thorough earthquake analyses shall be performed for all existing buildings in the area.
- TBEC (2018) [41] requires a site-specific elastic acceleration spectrum only for local soil class ZF. Although the code allows design engineers to request similar studies for other soil classes, there is no clear statement to justify this request. Thus, adding a statement to the code requiring a site-specific elastic acceleration spectrum in areas like Bayraklı would help meet earthquake design needs.
- In order to prevent any further loss of life and property during future earthquakes, a detailed earthquake hazard assessment should be prepared, specifically for buildings located in the İzmir Bay area.
- The fully and partially collapsed buildings in İzmir during the Aegean Sea earthquake were constructed when TEC (1975) [46] was in effect. However, many of the requirements in the code were not followed during the design or construction stages.
- Inspections during the design and construction phases were not performed properly for buildings constructed before 2000. Therefore, all the reinforced concrete buildings constructed in Turkey before 2000 should be reevaluated for their structural performance.
- Necessary administrative precautions should be taken to sustain the structural integrity of reinforced concrete buildings during their lifespans.

REFERENCES

[1] Sahin, B.E., Tunc, G., and Ozsarac, E., "Disaster Management and Public-Private Partnership in Turkey", International Civil Engineering and Architecture Conference, ICEARC19, 17-20 April 2019, Trabzon, Turkey.

[2] Aral, M., Tunc, G., "A Proposal for the Establishment of Building Identity Numbers in Turkey Based on the Performance of Buildings During Earthquakes", Journal of Disaster and Risk, 4(1), pp.20-41, 2021.

[3] MTA (General Directorate of Mineral Research and Exploration), https://www.mta.gov.tr/v3.0/hizmetler/yenilenmis-diri-fay-haritalari, last accessed 01.04.2022 (in Turkish).

[4] AFAD (Disaster and Emergency Management Authority): Preliminary evaluation report of October 30, 2020 Mw 6.6 Aegean Sea, Seferihisar (İzmir) Earthquake. Turkish Ministry of Interior, Department of Earthquake, Ankara, Turkey, 2020 (in Turkish).

[5] TÜİK (The Turkish Statistical Institute), https://www.tuik.gov.tr/, last accessed 01.04.2022 (in Turkish).
[6] AA (Anadolu Agency), https:// www.aa.com.tr/tr/turkiye/bakan-kurum-izmirde-tum-hasar-tespit-calismalar-tamamlandi/2039895, last accessed 01.04.2022 (in Turkish).
[7] Nuhoğlu A., Erener M.F. Hızal Ç., Kıncal C., Erdoğan D.Ş., Özdağ Ö.C., Akgün M., Ercan E., Kalfa E., Köksal D., İpek Y., and Sezer A."A reconnaissance study in Izmir (Bornova Plain) affected by October 30, 2020 Samos earthquake", International Journal of Disaster Risk Reduction, 63 (2021) 102465, https://doi.org/10.1016/j.ijdrr.2021.102465.
[8] Cetin K.O., Altun S., Askan A., Akgün M., Sezer A., Kıncal C., Özdağ Ö.C., İpek Y., Unutmaz B., Gülerce Z., Özacar A., Ilgaç M., Can G., Cakir E., Söylemez B., El-Sayeed A., Zarzour M., Bozyiğit İ., Tuna Ç., Köksal D., Karimzadeh S., Uzel B., Karaali E., "The site effects in Izmir Bay of October 30 2020, M7.0 Samos Earthquake", Soil Dynamics and Earthquake Engineering, 152 (2022) 107051, https://doi.org/10.1016/j.soildyn.2021.107051.
[9] Akinci A., Cheloni d., Dindar A.A. "The 30 October 2020, M7.0 Samos Island (Eastern Aegean Sea) Earthquake: effects of source rupture, path and local-site conditions on the observed and simulated ground motions" Bulletin of Earthquake Engineering (2021) 19:4745–4771. https://doi.org/10.1007/s10518-021-01146-5 .
[10] Makra K., Rovithis E., Riga E., Raptakis D., Pitilakis K. "Amplification features and observed damages in İzmir (Turkey) due to 2020 Samos (Aegean Sea) earthquake: identifying basin effects and design requirements", Bulletin of Earthquake Engineering (2021) 19:4773–4804. https://doi.org/10.1007/s10518-021-01148-3 .
[11] Demirci, H.E., Karaman M., Bhattacharya S. "A survey of damage observed in Izmir due to 2020 Samos-Izmir earthquake", Natural Hazards (2022) 111:1047–1064, https://doi.org/10.1007/s11069-021-05085-x.
[12] Binici B., Yakut A., Canbay E., Akpinar U., Tuncay K. "Identifying buildings with high collapse risk based on samos earthquake damage inventory in İzmir" Bulletin of Earthquake Engineering, https://doi.org/10.1007/s10518-021-01289-5.
[13] Demir A., Altıok T.Y. "Numerical assessment of a slender structure damaged during October 30, 2020, İzmir earthquake in Turkey" Bulletin of Earthquake Engineering (2021) 19:5871–5896, https://doi.org/10.1007/s10518-021-01197-8.
[14] Yakut A., Sucuoğlu H., Binici B., Canbay E., Donmez C., İlki A., Caner A., Celik O.C., Ay B.Ö. "Performance of structures in İzmir after the Samos island earthquake", Bulletin of Earthquake Engineering, September 2021, https://doi.org/10.1007/s10518-021-01226-6.
[15] "Global Catastrophe Recap: November 2020" by EON, http://thoughtleadership.aon.com/Documents/20201210_analytics-if-november-global-recap.pdf, last accessed 01.04.2022.
[16] Okay, A.I., Zattın, M., Cavazza. W.: Apatite fissiontrack data for the Miocene Arabia-Eurasia collision, Geology (38), pp. 35-38, 2010.
[17] Kuruoglu, M., Eskisar, T.: Effect of local soil conditions on dynamic ground response in the southern coast of Izmir Bay, Turkey, Russian Geology and Geophysics (56), pp. 1201–1212, 2015.
[18] Drahor, M.G., Berge, M.A.: Integrated geophysical investigations in a fault zone located on southwestern part of İzmir city, Western Anatolia, Turkey, Journal of Applied Geophysics (136), pp. 114–133, 2017.
[19] Emre, Ö., Barka, A.: Active faults between Gediz Graben and Aegean Sea (İzmir Region), Earthquake Symposium for Western Anatolia, İzmir, Turkey, pp. 131–132, 2000 (in Turkish).
[20] Ocakoğlu, N., Demirbağ, E., Kuşcu, İ.: Neotectonic structures in the area offshore of Alaçatı, Doğanbey and Kuşadası (western Turkey): Evidence of strike-slip faulting in the Aegean extensional province, Tectonophysics (391), pp. 67–83, 2004.
[21] Ocakoğlu, N., Demirbağ, E., Kuşçu, İ.: Neotectonic structures in İzmir Gulf and surrounding regions (western Turkey): Evidences of strike-slip faulting with compression in the Aegean extensional regime, Marine Geology (219), pp. 155–171, 2005.
[22] Emre, Ö., Özalp, S., Doğan, A., Özaksoy, V., Yıldırım, C., Göktaş, F.: Active faults in the vicinity of Izmir and their earthquake potential, Report No: 10754, General Directorate of Mineral Research and Exploration, Ankara, Turkey, 2005 (in Turkish).

[23] Altun, S., Sezer, A., Göktepe, A.B.: A preliminary microzonation study on Northern Coasts of Izmir: Investigation of the local soil conditions, Soil Dynamics and Earthquake Engineering (39), pp. 37–49, 2012.
[24] Ketin, I.: Türkiye'nin genel tektonik durumu ile baslıca deprem bölgeleri arasındaki ilişkiler, Bulletin of Mineral Research and Exploration (71), pp. 129–134, 1969 (in Turkish).
[25] Bozkurt, E.: Neotectonics of Turkey - A Synthesis, Geodinamica Acta (14), pp. 3–30, 2001.
[26] Aksu, A.E., Piper, D.J.W., Konuk, T.: Late Quaternary tectonic and sedimentary history of outer İzmir and Candarli bays, Western Turkey, Marine Geology (76), pp. 89–104, 1987.
[27] Sozbilir, H., Uzel, B., Sumer, O., Inci, U., Ersoy, E., Kocer, T., Demirtas, R., Ozkaymak, C.: Data about coordinated working of the E-W oriented Izmir Fault and the NE-SW oriented Seferihisar Fault: Kinematical and paleoseismological studies on active faults occurring gulf of Izmir, Western Anatolia, Bulletin of Turkish Geology (52), pp. 91–114, 2008 (in Turkish).
[28] Sozbilir, H., Sumer, O., Uzel, B., Ersoy, E., Erkul, F., Inci, U., Helvaci, C., Ozkaymak, C.: Seismic geomorphology of October 17–20, 2005 Sigacik Bay earthquakes and relation with stress areas in region, Western Anatolia, Bulletin of Turkish Geology (53), pp. 217–238, 2009 (in Turkish).
[29] Uzel, B., Sozbilir, H., Ozkaymak, C.: Evolution of an actively growing superimposed basin in Western Anatolia: The Inner Bay of Izmir, Turkish Journal of Earth Sciences (21), pp. 439–471, 2012.
[30] Kıncal, C.: Evaluation of geological units in İzmir inner bay and its vicinity by using GIS and remote sensing systems in terms of engineering geology, PhD Thesis, Dokuz Eylül University, 2004 (in Turkish).
[31] Pamuk, E., Özdağ, Ö.C., Akgün, M.: Soil characterization of Bornova Plain (Izmir, Turkey) and its surroundings using a combined survey of MASW and ReMi methods and Nakamura's (HVSR) technique, Bulletin of Engineering Geology and the Environment (78), pp. 3023–3035, 2019.
[32] AFAD (Disaster and Emergency Management Authority), Turkish Ministry of Interior, Ankara, https://tdth.afad.gov.tr/, last accessed 01.04.2022 (in Turkish).
[33] MTA (General Directorate of Mineral Research and Exploration), http://yerbilimleri.mta.gov.tr/anasayfa.aspx, last accessed 01.04.2022 (in Turkish).
[34] Pamuk, E., Akgün, M., Özdağ, Ö.C., Gönenç, T.: 2D soil and engineering-seismic bedrock modeling of eastern part of Izmir inner bay/Turkey, Journal of Applied Geophysics (137), pp. 104–117, 2017.
[35] KOERI (Kandilli Observatory and Earthquake Research Institute): October 30, 2020 Aegean Sea Earthquake Press Bulletin, Boğaziçi University, Istanbul, Turkey, 2020 (in Turkish).
[36] USGS (The United States Geological Survey) https://earthquake.usgs.gov/earthquakes/eventpage/us7000c7y0/executive, last accessed 01.04.2022.
[37] CMT (Harvard), https://www.globalcmt.org/ , last accessed 01.04.2022.
[38] GFZ , https://geofon.gfz-potsdam.de/, last accessed 01.04.2022.
[39] MTA (General Directorate of Mineral Research and Exploration): Field Observations and Evaluation Report of October 30, 2020 (M_w=6.6) Aegean Sea Earthquake, Turkish Ministry of Energy and Mineral Resources, Ankara, Turkey, 2020 (in Turkish).
[40] METU (Middle East Technical University): Seismic and structural damages related to site observations for the October 30, 2020 Samos Island (off the coast of Seferihisar, İzmir) Earthquake, Report No: ODTÜ/DMAM 2020-03, Ankara, 2017 (in Turkish).
[41] Ministry of Environment and Urban Planning: Turkish Building Earthquake Code (TBEC), Ankara, Turkey, 2018 (in Turkish).
[42] AFAD (Disaster and Emergency Management Authority): Turkish Ministry of Interior, Ankara, Turkey https://deprem.afad.gov.tr/istasyonlar, last accessed 01.04.2022 (in Turkish).
[43] Metropolitan Municipality of Izmir, Izmir City Guide Building Count Distribution Map, https://kentrehberi.izmir.bel.tr/izmirkentrehberi#, last accessed 01.04.2022 (in Turkish).
[44] METU, The Samos (İzmir-Seferihisar Offshore) Earthquake [30 October 2020 Mw=6.6] Field Observations On Seismic and Structural Damage, Earthquake Engineering Research Center, Middle East Technical University, Report No: METU/EERC 2020–03, November 2020.
[45] Ministry of Public Works and Settlement: Italian building instructions in earthquake districts (TEC), Ankara, Turkey, 1940 (in Turkish).

[46] Ministry of Public Works and Settlement: Specification for structures to be constructed in disaster areas (TEC), Ankara, Turkey, 1975 (in Turkish).
[47] Ministry of Public Works and Settlement: Specification for structures to be constructed in disaster areas (TEC), Ankara, Turkey, 1998 (in Turkish).
[48] Ministry of Public Works and Settlement: Specification for buildings to be constructed in earthquake areas (TEC), Ankara, Turkey, 2007 (in Turkish).
[49] Bayraklı Municipality, Earthquake Investigation Center, İzmir, Turkey, https://bayrakli.bel.tr/Sayfa/80/deprem-etud-merkezi-baydem, last accessed 01.04.2022 (in Turkish).
[50] AA (Anadolu Agency) Ankara, Turkey, https://www.aa.com.tr/tr/turkiye/bayrakli-belediye-baskani-sandaldan-rizabey-ve-doganlar-apartmanlari-raporuyla-ilgili-aciklama/2030535, last accessed 01.04.2022 (in Turkish).
[51] Mertol H.C., Tunc G., Akis T. "Damage Observation of Reinforced Concrete Buildings after 2020 Sivrice (Elazığ) Earthquake, Turkey", Journal of Performance of Constructed Facilities, 2021, 35(5): 04021053, https://doi.org/10.1061/(ASCE)CF.1943-5509.0001619
[52] Karakus, K. Geological soil reports and legal regulations. Ankara, Turkey: Chamber of Geological Engineers, 2009.
[53] Nuhoğlu A., Erener M.F. Hızal Ç., Kıncal C., Erdoğan D.Ş., Özdağ Ö.C., Akgün M., Ercan E., Kalfa E., Köksal D., İpek Y., and Sezer A. "A reconnaissance study in Izmir (Bornova Plain) affected by October 30, 2020 Samos earthquake", International Journal of Disaster Risk Reduction, 63 (2021) 102465, https://doi.org/10.1016/j.ijdrr.2021.102465
[54] Demirci, H.E., Karaman M., Bhattacharya S. "A survey of damage observed in Izmir due to 2020 Samos-Izmir earthquake", Natural Hazards (2022) 111:1047–1064, https://doi.org/10.1007/s11069-021-05085-x

[55] Radnić, J., Grgić, N., Buzov, A., Banović, I., Smilović Zulim, M., Baloević, G., Sunara, M.: Mw 6.4 Petrinja earthquake in Croatia: Main earthquake parameters, impact on buildings and recommendation for their structural strengthening, *GRAĐEVINAR, 73* (2021) 11, pp. 1109-1128, doi: https://doi.org/10.14256/JCE.3243.2021
[56] Mertol, H. C., Tunc, G., Akis, T.: Evaluation of masonry buildings and mosques after Sivrice earthquake, *GRAĐEVINAR, 73* (2021) 9, pp. 881-892, doi: https://doi.org/10.14256/JCE.3101.2021
[57] Šavor Novak, M., Uroš, M., Atalić, J., Herak, M., Demšić, M., Baniček, M., Lazarević, D., Bijelić, N., Crnogorac, M., Todorić, M.: Zagreb earthquake of 22 March 2020 – preliminary report on seismologic aspects and damage to buildings, *GRAĐEVINAR, 72* (2020) 10, pp. 843-867, doi: https://doi.org/10.14256/JCE.2966.2020